Design of a Compact Wideband Balun Bandpass Filter with High Selectivity

Hui Ma, Jiayuan Lu, Yuran Li, Lin Liu, and Jianpeng Wang

Nanjing University of Science and Technology, Nanjing 210094, China
hui644909@163.com, eejylu@njust.edu.cn, eeyuranli@163.com, eelinliu@163.com, eejpwang@gmail.com

Abstract **─** A new design method for compact wideband balun bandpass filter (BPF) with high selectivity is proposed in this paper. To achieve wide operation bandwidth, the first three resonant modes, i.e., one odd mode and two even modes, of a folded stepped-impedance multi-mode resonator are utilized and arranged inside the passband. Then, to realize good balance-to-unbalance performance, a microtrip to coplanar stripline transition structure is introduced in the design. Finally, a balun BPF characterized with both wide bandwidth and high selectivity has been eventually achieved through proper coupling topology. Besides, to further demonstrate the validity of our design concept, a practical microstrip wideband balun BPF with the fractional bandwidth (FBW) of 66% and two respective transmission zeros located at 1.4 GHz and 4.2 GHz is designed, fabricated, and measured. As expected, both the simulated and measured results exhibit good filtering and balun performance.

Index Terms **─** Balun Bandpass Filter (BPF), microstrip, multi-mode resonator, wide bandwidth.

I. INTRODUCTION

Recently, the rapid development of modern wireless communication system has put forward higher requirements on RF devices with low cost, high performance, as well as miniaturization, simultaneously. In order to accommodate to this tendency, the research on multiple function embedded component is meaningful. A typical work according to this tendency is the study on the balun BPF. The balun BPF is actually a balun embedded bandpass filter as it possesses both the functions of the balun and the bandpsss filter, which are both key components in RF front-end systems. Specifically, the balun BPF can not only provide a frequency selectivity of a bandpass filter, but also can maintain a function of balance-to-unbalanced conversion. Over the past few years, various balun BPFs with high performance have been explored in [1-9].

Based on the lumped-elements, baluns with significantly size reduction were proposed in [1]. However, it limits the application to higher frequency due to the inherent increased parasitic effect of the lumped elements. Meanwhile, the low temperature co-fired ceramic (LTCC) technology also shows its advantage on size reduction in the design of balun BPF due to its multi-layer structure [2]. In order to realize both the low cost and good phase balance performance, balun BPFs were proposed by Chen et al. in [3] and Shao et al. in [4], according to the inherent wideband out-of-phase property of the DSPSL structure. However, the spacing between the two layer PCB structures could significantly influence the phase balance performance. Besides, based on the electrical field distribution of the multi-mode resonator, various types of balun BPFs are designed with a variety of multi-mode resonators, such as the loop resonator in [5], the open loop resonator in [6]， the patch resonator in [7], the SIW resonator in [8], and the hybrid resonator in [9]. Although both characteristics of balun and bandpass filter can be realized, it is hard to realize the wideband performance as only the odd resonant modes can be utilized in the design according to this introduced method. Therefore, to the best knowledge, it is still a very challenging work to develop a compact balun BPF with both the performances of wide operation bandwidth and high selectivity.

The primary motivation of this paper is to design a compact balun BPF which can not only provide wideband response but also maintain high selectivity performance. For this purpose, a microstrip to coplanar stripline transition structure is proposed in order to realize the desired balance-to-unbalance conversion performance in the design initially. Then, the resonant properties of the employed folded stepped-impedance multi-mode resonator are studied. Afterwards, a wideband balun BPF with high selectivity has been successfully achieved through proper coupling topology. Finally, both simulated and measured results of the presented balun BPF are provided and good agreement between them is gained to demonstrate good experimental validation.

II. ANALYSIS AND DESIGNN OF THE PROPOSED BALUN BPF

A. Balun structure design

Figure 1 shows the top view and bottom view of

Submitted On: January 12, 2016
Accepted On: March 18, 2016

the proposed balun BPF respectively. As indicated in the Fig. 1, the proposed balun BPF is mainly composed of two sections, i.e., part A and part B. For part A in Fig. 1, it is constructed by the microstrip to coplanar stripline transition and plays the role of balun function. Specifically, the transition form is realized by connecting the ground plane of the microstrip line with one of the coplanar striplines (line S in Fig. 2) through shorting via-holes.

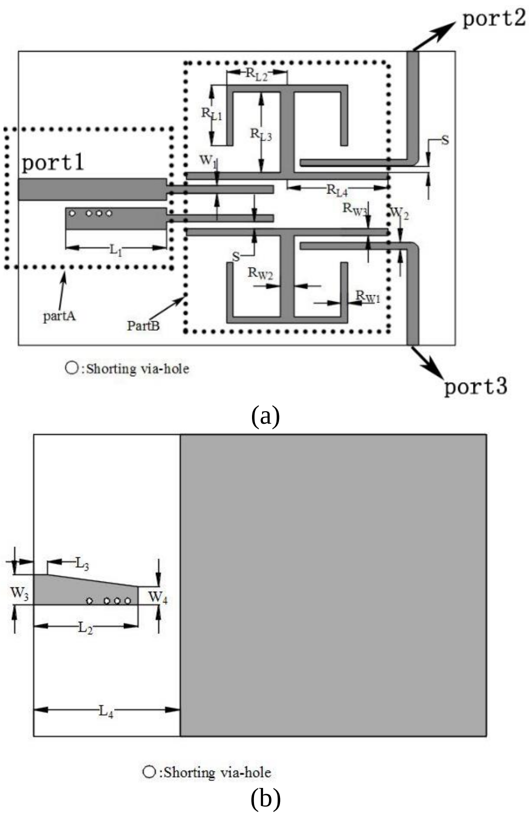

Fig. 1. Layout of the wideband balun BPF: (a) top view and (b) bottom view.

The coplanar stripline structure adopted here aims to achieve wideband phase and magnitude balance performance in the balun design. To illustrate the operation principle of the balun structure, electric field distributions referring to different cross-sections indicated in the transitions are displayed in Fig. 2.

As we can see from Fig. 2, when an unbalanced signal is initially fed into the microstrip line of the transition structure at the A-A' section, the electric fields are perpendicularly terminated at the ground of the substrate as depicted in Fig. 2 (b1). After the signal coming into the transition section, the electric fields at the section B-B' are displayed accordingly in Fig. 2 (b2). It shows that at the transition section B-B' the electric fields are terminated both at the back ground plane and one of the lines of the coplanar stripline which are bonding together by the introduced via holes. Owing to the transition structure, the unbalanced signal has successfully propagated along the coplanar stripline with the electric fields at the section C-C' displayed in Fig. 2 (b3). Finally, by introducing the back ground and decreasing the coupling between the coplanar stripline, the unbalanced signal transmits through the coplanar stripline will be eventually divided into a pair of balanced signals. As can be seen, the electric fields at the E-E' section in Fig. 2 (b4) for line M and line S are opposite, which means an 180° phase difference. Therefore, when an unbalanced signal is transmitted through the proposed transition circuit, a pair of balanced signals will be achieved at the two balanced outputs. Moreover, due to the inherent wideband property of the microstip-coplanar striplines transition, the proposed balun with wideband performance is promising.

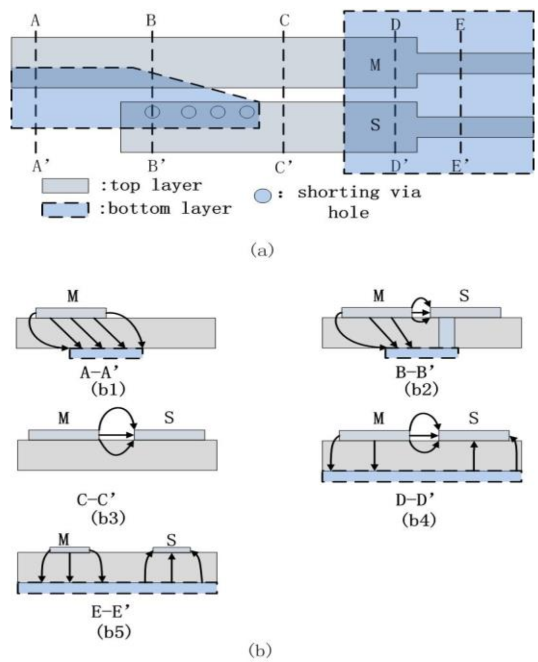

Fig. 2. Electrical field distributions on different cross-section: (a) sections in part A and (b) electric fields at different sections.

B. Filter part design

The filtering function is mainly achieved via the coupling between the balanced microstrip feed line and the presented multi-mode resonator shown in Part B of Fig. 1. As the bandwidth of the filter is mainly determined by the resonance of the multi-mode resonator, here, we will analyze it in detail. The configuration of proposed resonator is shown in Fig. 3. Since the resonator is symmetrical with respect to the symmetry plane, the well-known even- and odd-mode method is applied. Figure 3 also illustrates the equivalent circuits of the resonator under the even- and odd-mode excitation. The input admittance can be derived as:

$$Y_{inodd} = Y_1 / (j \tan\theta_1), \tag{1}$$

$$Y_{ineven} = Y_1 \frac{Y_L + jY_1 \tan\theta_1}{Y_1 + jY_L \tan\theta_1}, \tag{2}$$

where

$$Y_L = \mathrm{j}\frac{Y_2}{2} \cdot \frac{(Y_2/2)\tan\theta_2 + Y_3 \tan\theta_3}{Y_2/2 - Y_3 \tan\theta_2 \tan\theta_3}. \tag{3}$$

For simplification, we set Y_2=2Y_3. Besides, tanθ_1, tanθ_2 and tanθ_3, approximately have the same value. Under the condition of resonance, it occurs when Y_{ineven}=Y_{inodd}=0. Thus, Equation (1) and (2) can be expressed as:

$$Y_1 / (\mathrm{j}\tan\theta_1) = 0, \tag{4}$$

$$\frac{Y_3}{Y_1} = \frac{\tan^2\theta_2 - 1}{2}. \tag{5}$$

The above Equations (4) and (5) indicate that the odd- and even-mode resonant frequencies can be determined by θ_1 and the value of Y_3/Y_1. The first and the third resonant mode are even-mode, while the second mode is odd-mode. The even-mode resonant frequencies denoted by f_{r1} and f_{r2} are the first and second solutions of Equation (5). Therefore, the even-mode frequencies can be derived by a known R_{L3}. Figure 4 presents the influence of different Y_3/Y_1 on even-mode frequencies, which further reveals their relationship. By controlling the value of Y_3/Y_1, the bandwidth can be easily adjusted. As for the odd-mode resonance frequency f_{odd}, it is only determined by the electrical length of θ_1. Therefore, we can readily achieve a desired bandwidth by the values of Y_3/Y_1 and θ_1 properly selected.

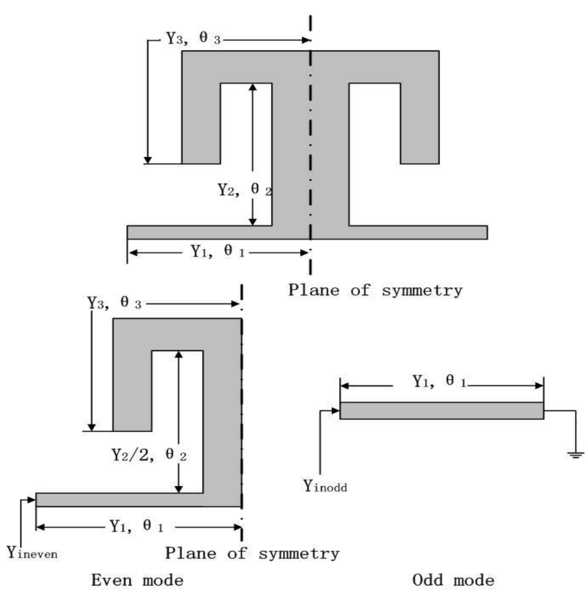

Fig. 3. Folded multi-mode resonator with it half bisections under odd- and even-mode excitation.

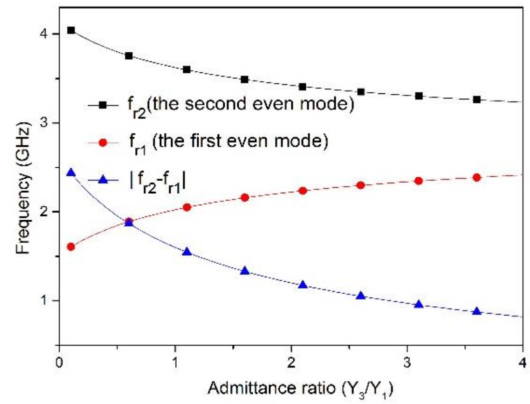

Fig. 4. Relationship between the admittance ratio and the even mode frequencies

III. SIMULATION AND MEASUREMENT RESULTS

To verify our design concept, one balun BPF sample is implemented by the method mentioned above. It is fabricated on a single layer substrate, i.e., Rogers RO4003C with a dielectric constant of 3.38, a loss tangent of 0.0027, and a thickness of 0.813 mm. The physical dimensions of the wideband balun BPF illustrated in Fig. 1 are as follows: L_1=18.5 mm, L_2=14 mm, L_3=4 mm, L_4=27.5 mm, W_1=0.6 mm, W_2=0.5 mm, W_3=3.6 mm, W_4=1.8 mm, R_{L1}=11.72 mm, R_{L2}=8.82 mm, R_{L3}=14.42 mm, R_{L4}=17.78 mm, R_{W1}=0.5 mm, R_{W2}=1.64 mm, R_{W3}=0.216 mm, S=0.1 mm.

The diameter of the via-hole is 0.8 mm. The photograph of the fabricated balun BPF is depicted in Fig. 5. Simulation was accomplished by the EM simulator HFSS 13.0 while the measurement was carried out on the Agilent N5244A.

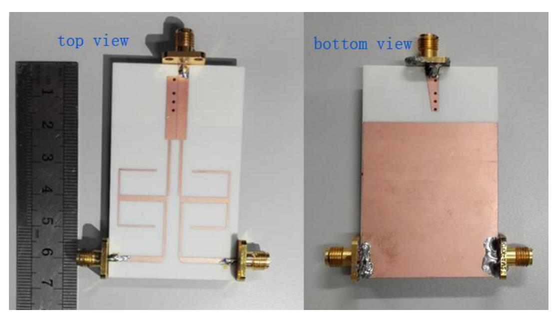

Fig. 5. Photograph of the wideband balun BPF.

The simulated and measured S-parameter parameters of the balun BPF are shown in Fig. 6. As indicated in the results, the designed balun BPF operates at the center frequency of 3.2 GHz with a fractional bandwidth (FBW) of 66%. Inside the whole passband, the insert loss is better than 1 dB and the return loss is better than 15 dB. Outside the passband, two transmission zeros located at 1.4 GHz and 4.2 GHz can be clearly observed, which ensure the proposed balun BPF a better than 25 dB suppression. The phase imbalance and the magnitude imbalance are shown in Fig. 7. It can be seen that good balance performance is achieved with amplitude imbalance of less than 0.5 dB and phase imbalance of better than 5°. It should be mentioned that the small discrepancy between measured and simulated results are mainly due to the fabrication tolerance and the insert loss of SMA connector. To sum up, the presented balun BPF performs well in high selectivity and ideal balance performance.

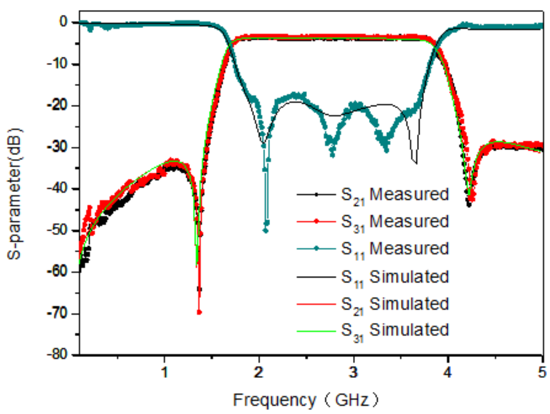

Fig. 6. Simulated and measured S-parameters of the proposed wideband balun BPF.

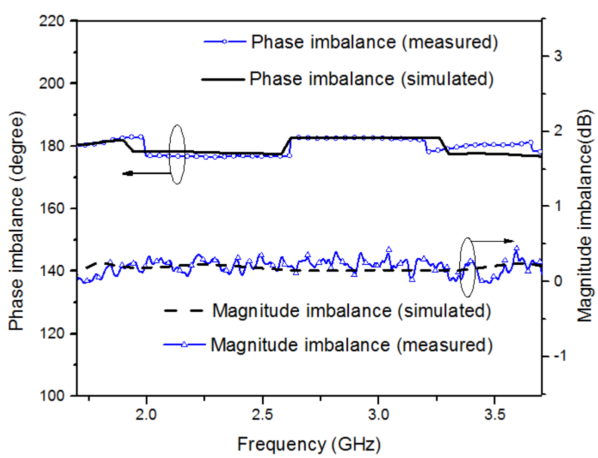

Fig. 7. Simulated and measured amplitude and phase imbalance in the passband.

IV. CONCLUSION

In this paper, a new method to design wideband balun BPF with high performance is proposed. To illustrate the design concept, both the operation principle of the balun circuit and the analysis of multi-mode resonator for the balun BPF are presented. One sample balun BPF is then designed and fabricated to validate the proposed design concept. As expected, the predicted results are well confirmed in experiment, thus validating that the presented wideband balun BPF is not only characterized by a good balance performance but also has high frequency selectivity. With these distinctive features, it is our belief that the developed balun BPF can be widely applied to modern advanced wideband wireless communication systems.

ACKNOWLEDGEMENT

This work was supported by the scientific research training fund (the BQW PLAN) of the Nanjing University of Science and Technology under Grant 201510288037.

REFERENCES

[1] V. G. Posadas, C. M. Pascual, J. L. J. Martín, and D. S. Vargas, "Lumped-element balun for UHF UWB printed balanced antennas," *IEEE Trans. Microw. Theory Tech.*, vol. 56, no. 7, pp. 2102-2107, Jul. 2008.

[2] C. H. Tsai, H. C. Chen, and T. L. Wu, "A novel compact balun using a weakly coupled line with grounded resonator," *IEEE Microw. Wireless Compon. Lett.*, vol. 24, no. 11, pp. 763-765, Feb. 2002.

[3] J. X. Chen, C. Y. Cheung, and Q. Xue, "Integrated bandpass filter balun based on double-sided parallel-strip line with an inserted conductor plane," *APMC Microw. Conf.*, Thailand, pp. 1-4, Dec. 2007.

[4] J. Shao, R. G. Zhou, C. Chen, X. H. Wang, H. Kim, and H. L. Zhang, "Design of a wideband balun using parallel strips," *IEEE Microw. Wireless Compon. Lett.*, vol. 23, no. 3, pp. 125-127, Mar. 2013.

[5] P. Cheong, T. S. Lv, W. W. Choi, and K. W. Tam, "A compact microstrip square-loop dual-mode balun-bandpass filter with simultaneous spurious response suppression and differential performance improvement," *IEEE Microw. Wireless Compon. Lett.*, vol. 21, no. 2, pp. 77-79, Feb. 2011.

[6] Q. Xue, J. Shi, and J. X. Chen, "Unbalanced-to-balanced and balanced-to-unbalanced diplexer with high selectivity and common-mode suppression," *IEEE Trans. Microw. Theory Tech.*, vol. 59, no. 11, pp. 2848-2855, Nov. 2011.

[7] S. Sun and W. Menzel, "Novel dual-mode balun bandpass filters using single cross-slotted patch resonator," *IEEE Microw. Wireless Compon. Lett.*, vol. 21, no. 8, pp. 415-417, Aug. 2011

[8] H. Chu and J. X. Chen, "Dual-band substrate integrated waveguide balun bandpass filter with high selectivity," *IEEE Microw. Wireless Compon. Lett.*, vol. 24, no. 6, pp. 379-381, June 2014.

[9] T. Yang, M. Tamura, and T. Itoh, “Compact hybrid resonator with series and shunt resonances used in miniaturized filters and balun filters,” *IEEE Trans. Microw. Theory Tech.*, vol. 58, no. 2, pp. 390-402, Feb. 2010

Hui Ma is working towards the Bachelor degree at Nanjing University of Science and Technology. Her research interests include the high performance multi-function microwave components.

Jiayuan Lu received the B.S. degree in Electronics and Information Engineering from NJUST, Nangjing, China, in 2014. He is currently working toward the Ph.D. degree in Electromagnetic Field and Microwave Technology in NJUST. His research interest is the design of miniaturized high performance microwave/millimeter-wave passive device and numerical methods in electromagnetics.

Yuran Li is working towards the Bachelor degree at Nanjing University of Science and Technology. Her research interests include the high performance multi-function microwave components.

Lin Liu is working towards the Bachelor degree at Nanjing University of Science and Technology. Her research interests include the high performance multi-function microwave components.

Jianpeng Wang received the M.Sc. and Ph.D. degree from UESTC, Chengdu, China, in 2004, and 2007, respectively. Since Jan. 2008, he has been with the Ministerial Key Laboratory of JGMT, School of Electronic and Optical Engineering, NJUST. His research interests include the high performance microwave/millimeter-wave passive components, circuits and systems realized on PCB, LTCC, etc.